On the Effect of Robotic Leg Design on Energy Efficiency *

Konstantinos Koutsoukis, *Student Member, IEEE*, Evangelos Papadopoulos, *Fellow, IEEE*

***Abstract*— In this paper, we study the effect of alternative leg designs on energy consumption in legged locomotion. Focusing on gaits with constant horizontal velocity and constant height we introduce models of two simplified parallel and serial designs with realistic mechanical and actuation parameters. The analysis yields the distribution of power demands in the leg workspace, leading to useful conclusions related to mechanical power antagonism and actuator electric losses. Mechanical antagonism occurs not only in parallel but also in serial legs causing extensive power waste, since one actuator contributes to the locomotion task and the other consumes power with no contribution to it. Based on the analysis, we propose a new leg design that minimizes the total actuation power consumption criterion given a nominal robot toe trajectory.**

I. Introduction

During the last decades, legged robots have made a giant leap forward. Exploiting their natural advantages over wheeled or tracked robots, such as increased mobility, agility and obstacle negotiation skills, legged robots have achieved astonishing locomotion performance by traversing challenging and discontinuous terrain, demonstrating dynamic running and performing highly dynamic maneuvers. Examples of robots with impressive capabilities include Boston Dynamics' Spot, and research quadrupeds such as ETH's ANYmal [1], equipped with novel compliant joint modules, IIT's hydraulic HyQ [2], and the MIT's Cheetah 3, using proprioceptive electric motors [3]. Despite the astonishing accomplishments in terms of mechanical/ electrical design and control, legged robots still feature energy efficiency significantly worse than animals of similar mass [4], [5]. Increasing energy efficiency is one of the last technical hurdles for making legged robots leave laboratory settings and operate in real life applications.

There have been several research attempts to improve energy efficiency. These can be classified to three main approaches: minimizing energy input by exploiting passive dynamics, storing energy in series elastic actuators (SEA), and minimizing the energy losses by using proprioceptive actuators. As far as passive dynamics is concerned Cornell's Ranger sets the stage in terms of energy efficiency by achieving a record cost of transport (CoT= 0.19) [6], [7]. However, this type of biped robot has sacrificed versatility to such an extent that it cannot perform any practical task.

The other approach for increasing energy efficiency makes use of SEA [8-11]. By integrating mechanical compliance between the gearbox output and the joint, roboticists primarily achieve motor and gearbox protection under dynamic interactions, while at the same time store temporarily energy and recover it using mechanical springs [12], [13]. In some cases, tunable stiffness of series elasticity is incorporated into geared motors of running robots [14], [15]. Incorporation of SEA in legged design led to robots like StarlETH with cost of transport (CoT=0.9), which is rather low when compared to other robotic devices of similar mass. However, SEA designs result in lower force bandwidth in comparison to designs without added compliance.

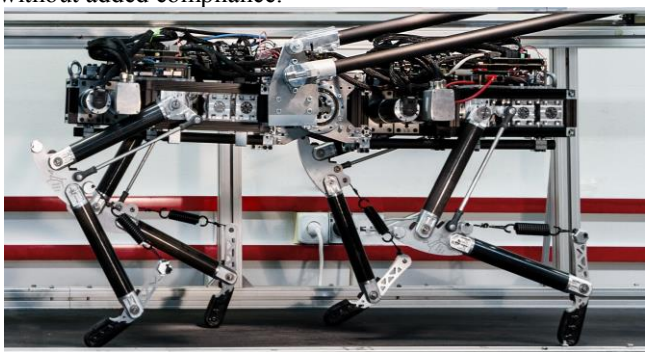

Figure 1. The quadruped robot Laelaps II, built by the Legged Robots Team at the Control Systems Lab of NTUA.

A more modern approach relied on the use of proprioceptive actuators [5], [16]. In this approach, energy losses are categorized into three types: actuator heat losses (including parasitic amplifier losses), transmission losses in the form of gear/belt/bearing friction losses, and interaction losses mainly due to foot impacts. Heat losses can be reduced significantly by custom high torque density motors [17], [18], and energy regeneration subsystems to recover energy during leg braking rather than dissipating it in form of Joule heating. Low impedance transmissions reduce transmission losses due to less stages used and allow energy flow between the actuator and the end effector in both directions. Finally, impact losses can be minimized by designing legs with lower distal mass, or by optimizing leg retraction [19]. Proprioceptive actuation schemes led to legged robots like the MIT Cheetah 3 with resulting cost of transport (CoT = 0.45 during trotting) which rivals running animals in the same scale [3].

In addition to above losses, in multi-actuator legged robots, poor energy efficiency is related also to "geometric work". The relation between mechanism geometry and mechanical efficiency was introduced in [20], but Waldron and Kinzel [21] originally discussed the idea of geometric work done by actuators acting as brakes. Song and Lee redefined geometric work as "the sum of the absolute values of the works by all actuators subtracted by the absolute value of the output work done by the system to the environment", so in cases where the actuators net output work is negative, forward driven actuators are the ones lowering energy efficiency [22]. For example, in the compliant biped ATRIAS, nearly all actuation power during normal operation is antagonistic, as a result of the pantograph leg design [23-25].

*This work was supported by the Hellenic Foundation for Research and Innovation (H.F.R.I.) under the "First Call for H.F.R.I. Research Projects to support Faculty members and Researchers and the procurement of high-cost research equipment grant" (Project Number: 2182)

Konstantinos Koutsoukis (e-mail: kkoutsou@central.ntua.gr), and Evangelos Papadopoulos (e-mail: egpapado@central.ntua.gr) are with the School of Mechanical Engineering, National Technical University of Athens, 15780 Athens, Greece.

In this paper we analyze the main sources of power consumption in case of both serial and parallel leg designs. The analysis includes realistic mechanical and electrical parameters (based on robot Laelaps II, see Fig. 1).We show that mechanical antagonism is related to task parameters and leg configuration and surprisingly occurs even in serial designs. Our spatial study, based on a given representative locomotion task, reveals the areas in the leg workspace where antagonism occurs and how leg design affects them.

The structure of the paper is as follows. In Section II we present the methodology employed by introducing the main dynamic models, determining the locomotion task and proceeding with justified simplifications. The spatial power consumption analysis for moderate speeds is presented in Section III. In Section IV the parallel leg design is modified to achieve minimum power consumption throughout a desired toe trajectory. Section V concludes the paper.

II. TROTTING WITH CONSTANT VELOCITY AT FIXED HEIGHT

A. Model description and parameters

We focus on the simplest planar leg architecture, consisting of 2 DoFs, the hip joint and the knee joint, and two main leg segments (upper and lower). We study the locomotion task during stance phase in terms of toe trajectory, focusing on toe trajectory with respect to robot's body (see Fig. 2). Instead of studying the leg in Fig. 2a, we study the dynamically and kinematically identical leg in Fig. 2b (assuming no sliding), and therefore, the toe trajectory during stance refers to Fig. 2b. The main design choice is related to the knee motor mounting, whether it will be mounted on the knee joint (serial leg design) or it will be mounted on the body (parallel leg design). We assume that both leg designs maintain the knee configuration during locomotion. Both designs will be subjects of this work in terms of energy efficiency.

A serial leg consists of two leg segments. The upper leg segment of mass m_1, inertia with respect to its Center of Mass (CoM) I_1 and length a_1, is connected via the hip joint to the robot main body. The distance between the CoM of the upper leg segment and the hip joint is denoted with l_1 (Fig.3) . The hip joint motor combo controls the joint angle θ_{1s} i.e. the angle between the segment and the robot body. The hip joint motor has mass mm_1, rotor inertia I_{r1}, resistance R_1, torque constant $K_{\tau 1}$ and gearbox inertia I_{g1} (w.r.t. motor shaft) and reduction ratio r_1 .The lower leg segment (mass m_2 , inertia w.r.t. its CoM I_2 , length a_2 and CoM-to-knee joint distance l_2) is connected to the upper leg segment with a knee joint. The knee joint motor combo is mounted on knee joint and actuates angle θ_{2s}, i.e. the angle between upper and lower leg segment. The knee motor combo consists of a motor of mass mm_2 , rotor inertia I_{r2} , resistance R_2 , torque constant $K_{\tau 2}$ and a gearbox of inertia I_{g2} (w.r.t. motor shaft) and reduction ratio r_2 .

In the case of parallel leg design (see Fig. 3) the model properties related to the hip joint are exactly the same. The only difference lies on the knee motor combo mounting, which is located on the robot's body and controls the angle θ_{2p} . The two transmission links are assumed to be massless.

The Coordinate System is attached to the hip joint, since the actual robot foot trajectories (x_e, y_e) are calculated with respect to the hip coordinate system. The forces exerted by the toe on the ground are denoted by F_e and the toe velocity is denoted by V_e. The model mechanical and electrical properties considered here correspond to the Laelaps II quadruped and are given in Table I.

The equations of motion for the two leg designs can be written in the following compact matrix form

$$\mathbf{M}_j(\mathbf{q}_j)\ddot{\mathbf{q}}_j + \mathbf{C}_j(\mathbf{q}_j,\dot{\mathbf{q}}_j)\dot{\mathbf{q}}_j + \mathbf{G}(\mathbf{q}_j) = \mathbf{T}_j - \mathbf{J}_j^T(\mathbf{q}_j)\mathbf{F}_e \quad (1)$$

where $\mathbf{M}$ is the mass matrix, matrix $\mathbf{C}$ contains Coriolis and centrifugal forces, $\mathbf{G}$ contains the gravitational terms and $\mathbf{J}$ is a Jacobian matrix. The index j takes values s in case of a serial leg or p in case of parallel leg. Angles, angular speeds and joint torques are denoted by $\mathbf{q}_j = [\theta_{1j}, \theta_{2j}]^T$, $\dot{\mathbf{q}}_j = [\dot{\theta}_{1j}, \dot{\theta}_{2j}]^T$ and $\mathbf{T}_j = [\tau_{1j}, \tau_{2j}]^T$ respectively. The force $\mathbf{F}_e$ is the ground reaction force.

TABLE I. MODEL MECHANICAL AND ELECTRICAL PROPERTIES

PARAMETER	VALUE	UNITS
Upper link length (α_1)	0.35	m
Lower link length (α_2)	0.35	m
Upper Leg CoM-to-hip distance (l_1)	0.175	m
Lower Leg CoM-to-hip distance (l_2)	0.175	m
Upper leg mass (m_1)	0.35	kg
Lower leg mass (m_2)	0.8	kg
Upper leg Inertia (I_1)	0.5262	kgm^2
Lower leg Inertia (I_2)	0.1644	kgm^2
Hip motor mass (mm_1)	1.150	kg
Knee motor mass (mm_2)	1.100	kg
Hip motor rotor inertia (I_{r1})	0.0000209	kgm^2
Knee motor rotor inertia (I_{r2})	0.0000542	kgm^2
Hip motor torque constant ($K_{\tau 1}$)	73.9	mNm/A
Knee motor torque constant ($K_{\tau 2}$)	93.4	mNm/A
Hip motor terminal resistance (R_1)	1.01	Ω
Knee motor terminal resistance (R_2)	0.608	Ω
Hip gearbox inertia–motor shaft (I_{g1})	0.00000173	kgm^2
Knee gearbox inertia–motor shaft (I_{g2})	0.00000172	kgm^2
Hip gearbox reduction ratio (r_1)	43	-
Knee gearbox reduction ratio (r_2)	53	-

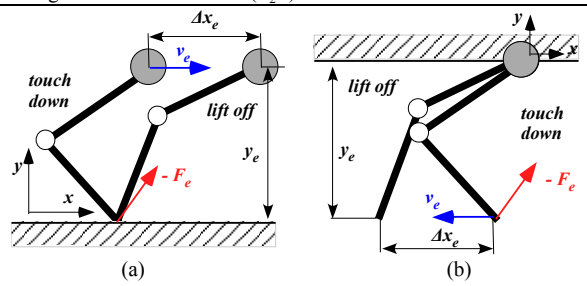

Figure 2. (a) Planar motion of a monoped with 2 segmented leg during stance phase. (b) Equivalent approach focusing on toe trajectory.

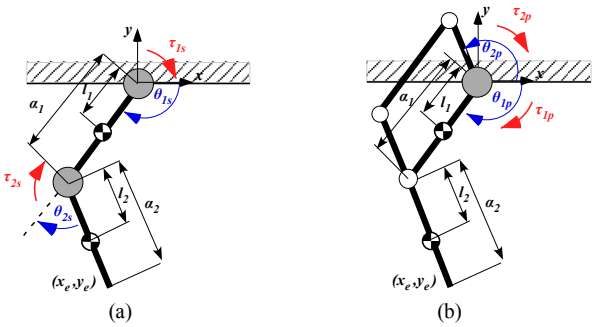

Figure 3. (a) Planar model of serial leg. (b) Planar model of parallel leg.

B. Locomotion Task

To gain insight on the effect on power consumption in a single legged system, we break down the generic locomotion task to its main building blocks. Each legged system has to:

(a) Successfully support its weight.
(b) Propel itself with the desired horizontal velocity.
(c) Maintain its desired height during locomotion.

Since the stance phase is the most energy demanding one during legged locomotion, we focus on this phase and examine some interesting points of the a-c building blocks.

To support the robot's body weight, an appropriate $\mathbf{F}_e$ must be applied. The vertical component of $\mathbf{F}_e$ is responsible for body support, whereas the horizontal component is related to horizontal acceleration/deceleration or/and friction losses compensation. In case of quadrupedal trotting without a flight phase, each leg supports half of the robot's weight.

As far as desired velocity and body height are concerned, we examine gaits with constant horizontal velocity and no height variations. Such gaits are produced by straight-line toe trajectories (during stance phase) and are widely used in actual quadruped robots and theoretical approaches [26], [27]. Since no acceleration/deceleration is taking place, the horizontal component of force $\mathbf{F}_e$ is compensating the friction losses only. Also, we focus on gaits with moderate horizontal velocity. The forces exerted on the environment are close to the forces applied by a leg during stance phases of a quadruped robot like Laelaps II, during moderate speed trotting [28],[29].

The locomotion task parameters and the desired toe trajectories are presented in Table II.

TABLE II. LOCOMOTION TASK PARAMETERS

PARAMETER	VALUE	UNITS
Toe horizontal velocity (V_{ex})	-1.0	m/s
Toe vertical velocity (V_{ey})	0.0	m/s
Force horizontal component (F_{ex})	-50.0	N
Force vertical component (F_{ey})	-200.0	N

C. Toe trajectories and inverse dynamics

In normal conditions, i.e. nominal locomotion with moderate speed, the robot's legs should not be extended to the end of their workspace. The toe trajectories should be as far from the workspace limits as possible. In this work, we set a 5% threshold for toe trajectory in order to take advantage of a relatively large portion of the available workspace.

The Jacobian matrix defines the mapping between the vector $\dot{\mathbf{q}}$ of joint/actuator velocities and the vector $\mathbf{V}_e$ of end-effector (toe) velocity

$$\mathbf{V}_e = \mathbf{J}_j(\mathbf{q}_j)\cdot\dot{\mathbf{q}}_j \tag{2}$$

If $\mathbf{J}_j(\mathbf{q})$ is full rank we can express the joint velocities with respect to the end-effector velocity $\mathbf{V}_e$ such that:

$$\dot{\mathbf{q}}_j = \mathbf{J}_j^{-1}\cdot\mathbf{V}_e \tag{3}$$

By differentiating (3) and taking into account that $\mathbf{V}_e$ is constant, we obtain the joint accelerations:

$$\ddot{\mathbf{q}}_j = (\dot{\mathbf{J}_j^{-1}})\cdot\mathbf{V}_e \tag{4}$$

To this end, combining (1), (3), (4) we can solve the inverse dynamics problem and calculate the joint torques in order for the toe to follow the desired trajectory with the desired speed.

III. POWER ANALYSIS

A. Total Actuation Power

The total actuation power P_{act} consumed by the actuators when the simplified leg performs the locomotion task is the sum of the mechanical power P_{mech} derived by the actuators plus the electric losses P_{el} at motor windings, i.e.:

$$P_{act} = P_{mech} + P_{el} = \sum_{i=1}^{2}\left|\tau_i\dot{\theta}_i\right| + \sum_{i=1}^{2} R_i\left(\frac{\tau_i}{K_{\tau i}r_i}\right)^2 \tag{5}$$

The mechanical power needed for each joint depends on the joint torque and angular speed whereas the electric losses depend only on torque demands and motor combo parameters such as motor resistance R_i, motor torque constant $K_{\tau i}$ and reduction ratio r_i. The gearbox power losses are omitted, and the motor torque is given by

$$\tau_{motor,i} = \tau_i / r_i \tag{6}$$

B. Mechanical Power

By setting the toe trajectory to be a straight horizontal line with constant velocity, we can perform a spatial analysis of the mechanical power needs at each point of leg's workspace. The importance of spatial analysis is that we can directly connect toe trajectories at the workspace of the leg with the power needed at each point of this trajectory, eliminating time.

For the mechanical parameters of Table I (coming from Laelaps II robot) and toe trajectory parameters of Table II, the dynamic terms of the equation of motion can be neglected since they are of lower order of magnitude than $\mathbf{T}_j$ and $\mathbf{J}_j^T(\mathbf{q}_j)\mathbf{F}_e$ for the workspace areas of interest. To this end, (1) can be simplified significantly, leading to a static relationship

$$\mathbf{T}_j = \mathbf{J}_j^T(\mathbf{q}_j)\mathbf{F}_e \tag{7}$$

As task we consider the trajectory of force – velocity pairs at end-effector ($\mathbf{F}_e$ - $\mathbf{V}_e$). The power requirements for this task can be calculated as:

$$P_{task} = \mathbf{F}_e\cdot\mathbf{V}_e \tag{8}$$

The net power of the leg's actuators for performing the aforementioned task is:

$$P_{net} = \sum_{i=1}^{2}\tau_i\cdot\dot{q}_i \tag{9}$$

The total mechanical power consumed by the actuators during the task, i.e. exerting $\mathbf{F}_e$ along the trajectory, while the toe is moving w.r.t. the body with velocity $\mathbf{V}_e$ is:

$$P_{mech} = \sum_{i=1}^{2}\left|\tau_i\cdot\dot{q}_i\right| \tag{10}$$

Combining (5) and (7)-(9) we reach to the conclusion that:

$$\left|P_{task}\right| = \left|P_{net}\right| \le P_{mech} \tag{11}$$

Net power calculation discards useful information concerning the overall manipulator efficiency since positive and negative powers cancel each other. Actuator powers that share the same sign with P_{task} contribute to the task whereas powers with the opposite sign consume power without contributing to the task, requiring other actuator to compensate.

The mechanical antagonism can be sufficiently studied through the simulation results of the two main leg designs for the toe trajectory parameters of Table II. For both designs the task net power equals 50 W since each leg moves on a

horizontal trajectory with constant velocity $V_{ex} = 1m/s$ and exerts the desired force $F_{ex} = 50N$ to the ground.

The total mechanical power for the serial and parallel leg designs are depicted in Fig 4, for an extended area of its workspace i.e. away from singularities and allowing sufficient distance from the hip joint for practical reasons. Each toe position is colored according to the mechanical power P_{mech} needed in order for the leg to perform the specific task of Table II.

Despite the fact that total mechanical power for the given task varies significantly throughout the workspace, it equals the task power requirements only in a limited area of the workspace, where no antagonism between the leg actuators occurs and therefore, where the mechanical power is minimum (see Eq.11). The remaining area, which is relatively large, is the area where the actuators contribute to the task with power of opposite sign, so that the net power equals the task power requirements but the total mechanical power of the actuators is much larger than the task power.

Fig. 5 shows the different workspace areas in terms of antagonism for the two alternative leg designs. As shown in Fig. 5, the non-antagonistic area of the workspace for the given parameters consists of two sub-areas, A1 and A2. These areas are limited by the curves C1, C2 and C3, C4, see Fig. 5. Interestingly, these curves correspond to the points of workspace where joint torque or joint angular speed equals zero and their location in the workspace depends only on the force and velocity direction and not their magnitude.

In more detail, across curve C1 knee torque equals zero. The same connection holds between curve C2 and hip angular velocity, curve C3 and hip torque, and finally between curve C4 and knee angular velocity. One can derive the analytical expressions of the curves, based on (3) and (7). Across the aforementioned curves, the power contribution of one of the actuators is zero while the other actuator is producing all the necessary power needed for the task. Since knee torque and hip angular velocity equal zero for the same configurations, curves C1 and C2 for both designs are located to the exact same position in leg workspace.

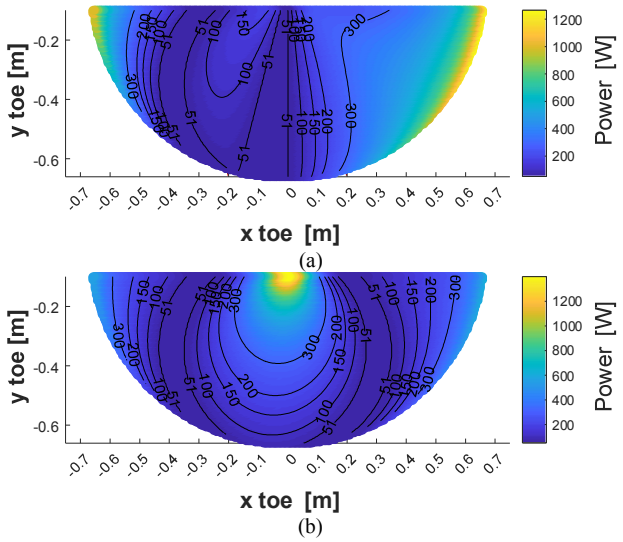

Figure 4. Total mechanical power over the workspace for the specified horizontal toe trajectory for (a) Planar model of serial leg design. (b) Planar model of parallel leg design. Isolines correspond to points with constant mechanical power consumption.

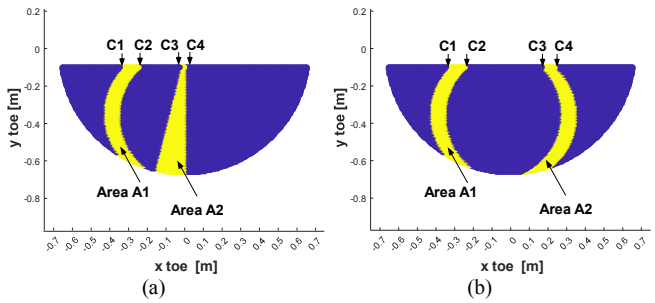

Figure 5. Areas of the workspace where mechanical antagonism occurs (blue areas) and non-antagonistic areas (yellow areas) for (a) Planar model of serial leg design. (b) Planar model of parallel leg design.

It is noted that mechanical antagonism occurs in both leg designs, and not only in the parallel leg design. It is closely connected to both leg design and task parameters, i.e. for the same leg design the areas will be removed correspondingly in the leg workspace in case of locomotion task change. To the best of the authors' knowledge, mechanical power antagonism has not been related previously to a serial leg design and the connection between mechanical power antagonism and task parameters has not been analyzed.

Comparing the locations of the non-antagonistic areas, in series and parallel design, see Fig. 5, one can easily notice that in case of serial design, a large non-antagonistic area lies below the hip joint (A2) whereas the corresponding areas in the case of parallel leg are located symmetrically (due to the equality between the lengths of upper and lower leg) around the hip (A1 and A2).

C. *Actuation Electric Losses*

As far as the electric losses of the actuators are concerned, the two designs result in different spatial distributions. The optimal area for the serial leg design is lower and lies on a relatively small area whereas the optimal area for the parallel leg design (featuring higher values compared to serial leg) presents minimum variation across toe horizontal trajectories.

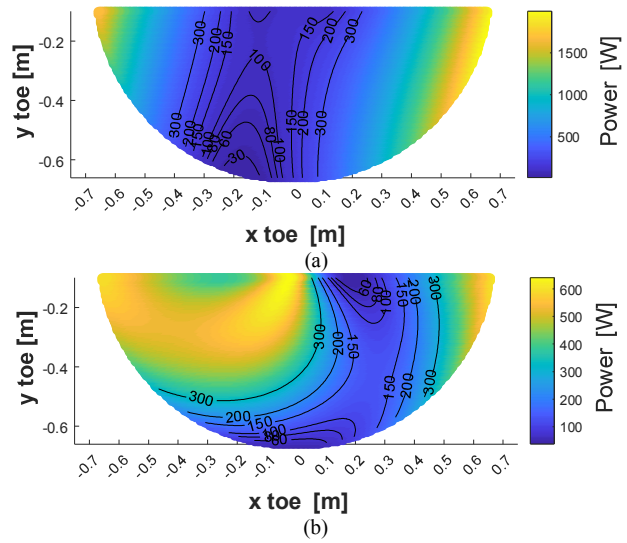

Figure 6. Motor electrical losses over the workspace for horizontal toe trajectory for (a) Planar model of serial leg design. (b) Planar model of parallel leg design. Isolines correspond to points with constant electrical losses.

Electric losses are of the same magnitude as mechanical power, so their contribution to total power consumption cannot be neglected. Another key feature of the electric losses is that they are closely related to the toque demands of each locomotion task, see (5).

IV. Increasing Energy Efficiency

A. Leg design

In the previous section, we focused on the different spatial power distribution among the serial and the parallel leg design. Leveraging the knowledge related to mechanical power antagonism and the electric losses, we propose a new leg design that minimizes the total actuation power consumption given a nominal robot toe trajectory. The new leg design is based on the parallel one, with the main difference that it incorporates a five-bar linkage for knee actuation, instead of a parallelogram, see Fig. 7.

By keeping the same leg architecture and segmentation (lengths for the upper and lower leg with the previous analysis), we highlight the impact of the knee transmission mechanism to power spatial distribution and efficiency.

Since the chosen linkage consists of a zero-length link (due to the coaxial motor placement of knee and hip motors) we use four-bar linkage terms (i.e. crank, coupler link, rocker, ground link) to describe it. Among the various types of five-bar linkages, we focus on a "crank – rocker" linkage type with the link of length a ("crank"), mounted on the knee motor, being able to perform a full rotation and the link of length c ("rocker") oscillating between two end positions. The upper leg link acts as the "ground" link and the link connecting the crank and the rocker is the coupler link. The proposed design parameters are shown in Table III.

In this linkage, the variation between the link lengths introduces a transmission ratio, i.e. the ratio of hip joint angular speed (input) over knee joint angular speed (output)

$$\text{Transmission Ratio} = \frac{c \cdot \sin\gamma}{a \cdot \sin\beta} \tag{12}$$

where angles γ and β are defined in Fig. 7. The transmission ratio depends on the geometry of the linkage and is constantly changing during leg motion. The numerous geometric limitations (Grashof's Law, endpoints location, etc.) and the requirement for sufficient workspace lead us to the simple design decision to allow only the "crank" link length vary between certain values (Table III) whereas the lengths of the other links are constant throughout the analysis.

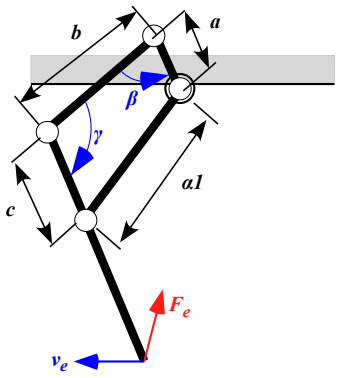

Figure 7. Generic case of 5 bar linkage for knee actuation.

TABLE III. Proposed Design Parameters

Parameter	Value	Units
Crank length (a)	0.01<0.1	m
Coupler link length (b)	0.35	m
Rocker link length (c)	0.1	m
Upper leg length (a_1)	0.35	m
Lower leg length (a_2)	0.35	m

B. Locomotion task parameters

The desired trajectory is symmetric with respect to the hip joint location (see Table IV) and is located away from the power-optimal areas A1 and A2 in case of the parallel leg design, and partially inside the A2 area in the case of the serial leg design (see Fig. 5).

TABLE IV. Toe Trajectory And Locomotion Task Parameters

Parameter	Value	Units
Toe Horizontal velocity (V_{ex})	-1.0	m/s
Toe Vertical velocity (V_{ey})	0.0	m/s
Force horizontal component (F_{ex})	-50.0	N
Force vertical component (F_{ey})	-200.0	N
Toe touchdown position (x_{etd},y_{etd})	(0.1,-0.55)	m
Toe distance traveled (Δx_e)	0.2	m
Toe lift off position (x_{elo},y_{elo})	(-0.1,-0.55)	m

However, for both designs, it lies in an area of relatively high actuation electric losses (Fig. 6). The force requirements are such that the leg can support the robot of body mass similar to the Laelaps II robot during trotting without flight phase. The max height of the trajectory is set to 0.55 m, leaving sufficient clearance for obstacle negotiation.

C. Performance index

The most widespread performance index related to energy efficiency is the Cost of Transport (CoT). Here, due to the focus on the stance phase, we evaluate the resulting designs using the Cost of Transport, CoT_{stance}, calculated during the stance phase only.

$$CoT_{stance} = \frac{E_{stance}}{mg\Delta x_e} \tag{13}$$

Where E_{stance} is the energy consumed by the actuators during stance i.e. the integral of total actuation power over time for the stance phase:

$$E_{stance} = \int_0^{T_{stance}} P_{act}\,dt \tag{14}$$

Since we focus on gaits with constant horizontal velocity and constant height, we can reform (14) as

$$E_{stance} = \frac{1}{v_{ex}} \int_0^{\Delta x_e} P_{act}\,ds \tag{15}$$

Taking into account (13-15) we finally have the proper expression for CoT_{stance}. This is defined as the integral of total actuation power over the distance traveled by the toe with respect to robot's body during stance phase, divided by the product of robot's mass, toe velocity, acceleration of gravity, and distance traveled during stance phase.

$$CoT_{stance} = (V_{ex} mg \Delta x_e)^{-1} \int_0^{\Delta x_e} P_{act} ds \quad (16)$$

D. Results

We calculate the actuation power and the CoT during stance for the geometrically acceptable five-bar linkage defined by the range parameters of Table III, and also for the serial and parallel leg designs which have been presented previously.

As far as the relationship between the CoT during stance and the crank length in the new leg design is concerned, our approach has led to an optimal crank length of 0.0383m which significantly reduces power demands across the desired trajectory (see Fig 8a). Parallel design (link a length equals 0.1m) features four times the stance CoT of the optimal design. The evolution of total actuation power for all three leg designs with respect to stance distance is depicted in Fig. 8b. The proposed design (with the optimal crank length) needs the lowest actuation power throughout the whole stance phase, whereas the serial leg design needs the most power just after touch down ($s = 0m$)and significantly lower power when it approaches the lift off event ($s = 0.2m$).

For the parallel leg design, the power requirements to perform the task are relatively stable during stance (240-370W) but significantly higher than the five-bar linkage leg. The values of stance CoT for the three leg designs for the certain locomotion task confirm the proposed leg design superiority in terms of energy efficiency ($CoT_{stance} = 0.397$).

TABLE V. PROPOSED DESIGN PARAMETERS

LEG DESIGN	COT STANCE
Serial Leg Design	1.223
Parallel Leg Design	1.596
5-Linkage Leg Design	0.397

The five-bar linkage leg design with the optimal crank length is depicted in Fig. 9 along with the resulting mechanical power antagonism areas in its workspace. As expected, the workspace of the leg has been reduced due to the crank-rocker type of the linkage. Interestingly the design choice made on the knee transmission mechanism had a significant result in the shape and location of A2, which has been reshaped and removed towards the task trajectory compared to the parallel leg design case (Fig. 5b).

In more detail, the relocation of curve C3, across which the torque of the hip motor equals zero is such that it has overcome curve C4 creating non-antagonistic Area 2 in the toe trajectory. This fact has a significant impact not only to the mechanical power demands but also to the actuation power losses related to the hip motor. The introduction of the nonlinear transmission ratio affected the force distribution throughout the leg resulting in extremely different hip motor torque demands.

As far as the functionality of the five-bar linkage is concerned the evolution of the angle γ during stance is depicted in Fig.10a. In order for a linkage of that type to operate smoothly over time the γ angle should vary between 40 and 120 degrees. For the proposed trajectory this condition is fulfilled. The resulting transmission ratio (see Fig.10b) should be taken into consideration since it results in higher knee motor angular speeds (and lower torque demands) when compared to parallel leg design.

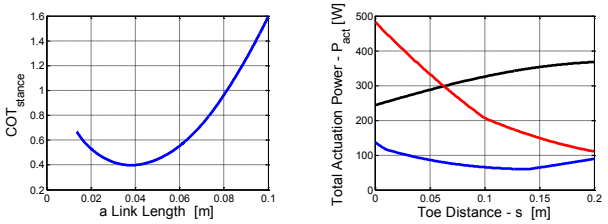

(a) (b)

Figure 8. (a) Evolution of the performance index for increasing crank link length. Length 0.1m corresponds to parallel leg design. (b) Evolution of total actuation power for 5-linkage leg with optimal crank link length (blue solid line), parallel leg (black solid line) and serial leg (red solid line).

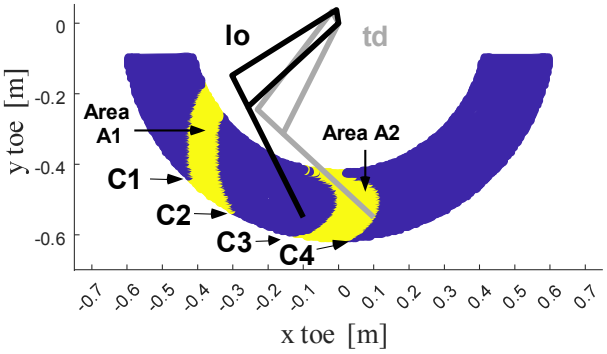

Figure 9. Areas of the workspace where mechanical antagonism occurs (blue areas) and non-antagonistic areas (yellow areas) for the 5-linkage leg design with the optimal crank link length. The leg configuration is depicted at the touch down (gray solid lines) and lift off (black solid lines). The red solid line corresponds to the trajectory of the toe during stance phase.

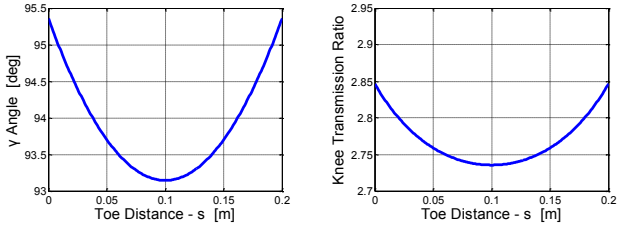

(a) (b)

Figure 10. Evolution of (a) γ angle and (b) the knee mechanism transmission ratio over travelled distance for the proposed leg design.

V. CONCLUSIONS AND FUTURE WORK

In this paper we analyzed the effect of leg design on mechanical power antagonism and actuation electric loses in gaits with constant horizontal velocity and constant height. Simplified leg models were introduced with realistic parameters and compared the spatial distribution of the power demands over their workspace for a specific locomotion task. Leveraging our understanding for the mechanism behind energy consumption in legged locomotion we introduced a new leg design, based on the parallel leg design, which features significantly reduced CoT_{stance} for the desired toe trajectory. These promising results will lead us to investigate further the use of this leg design in quadruped models with varying gait parameters (toe trajectory, toe velocity) and study also the impact of energy regeneration on leg design.

VI. REFERENCES

[1] Hutter, Marco, et al," ANYmal - A Highly Mobile and Dynamic Quadrupedal Robot," *Proceedings of the IEEE/RSJ International Conference on Intelligent Robots and Systems* (IROS), Daejeon, South Korea, 2016, pp.38-44.

[2] Semini, C., N. G. Tsagarakis, E. Guglielmino, M. Focchi, F. Cannella, and D. G. Caldwell, "Design of HyQ – a hydraulically and electrically actuated quadruped robot," *Proceedings of the Institution of Mechanical Engineers, Part I: Journal of Systems and Control Engineering*, vol. 225, no. 6, pp. 831–849, 2011.

[3] Bledt, G., M. J. Powell, B. Katz, J. Di Carlo, P. M. Wensing, and S. Kim, "MIT Cheetah 3: Design and Control of a Robust, Dynamic Quadruped Robot", *Proceedings of the IEEE/RSJ International Conference on Intelligent Robots and Systems* (IROS), Oct. 2018, pp.2245-2252.

[4] Tucker, V. A., "The energetic cost of moving about: Walking and running are extremely inefficient forms of locomotion. much greater efficiency is achieved by birds, fish and bicyclists," *American Scientist*, vol. 63, no. 4, pp. pp. 413–419, 1975.

[5] Seok, S., A. Wang, M.Y.M.. Chuah, D. Otten, J. Lang, and S. Kim, "Design principles for highly efficient quadrupeds and implementation on the MIT Cheetah robot," *Proceedings of the IEEE International Conference on Robotics and Automation (ICRA),* Karlsruhe, Germany, 2013, pp. 3292 – 3297.

[6] Bhounsule, P., J. Cortell, and A. Ruina, "Design and control of ranger:An energy-efficient, dynamic walking robot," in CLAWAR 2012 – *Proceedings of the Fifteenth International Conference on Climbing and Walking Robots and the Support Technologies for Mobile Machines*, July 2012, pp. 441–448.

[7] Ruina, A., (2012, September) "Cornell ranger 2011, 4-legged bipedal robot." [Online]. Available: http://ruina.tam.cornell.edu/research/topics/locomotion_and_robotics/ranger/Ranger2011/

[8] Pratt, G. A., and M. M. Williamson, "Series elastic actuators," *Proceedings of the IEEE/RSJ International Conference on Intelligent Robots and Systems*, 1995, vol. 1, pp. 399–406.

[9] Gregorio, P., M. Ahmadi, and M. Buehler, "Experiments with an electrically actuated planar hopping robot," in *Experimental Robotics* III. Berlin, Germany: Springer, 1994, pp. 267–281.

[10] Raibert, M. H., "Legged robots," *Commun. ACM*, vol. 29, no. 6, pp. 499–514, Jun. 1986.

[11] Hutter, M., C. Gehring, M. Hopflinger, M. Blosch, and R. Siegwart, "Toward combining speed, efficiency, versatility, and robustness in an autonomous quadruped," *IEEE Transactions on Robotics*., vol. 30, no. 6, pp. 1427–1440,Dec. 2014.

[12] Kim, S., J. Clark, and M. Cutkosky, "isprawl: Design and tuning forhigh-speed autonomous open-loop running," *The International Journal of Robotics Research*, vol. 25, no. 9, pp. 903–912, 2006.

[13] Hutter M, Remy CD, Hoepflinger MA, et al. "Efficient and versatile locomotion with highly compliant legs," *IEEE/ASME Transactions on Mechatronics*, 2013;18:449–458.

[14] Hurst, J. W., Chestnutt. J. E., and Rizzi, A. A., "An actuator with physically variable stiffness for highly dynamic legged locomotion", *Proc. of IEEE International Conference on Robotics and Automation*, New Orleans, LA, USA: IEEE, April 2004, pp. 4662-4667.

[15] Galloway, K., J. Clark, and D. Koditschek, "Design of a tunable stiffness composite leg for dynamic locomotion", in *ASME IDETC/CIE*, 2009.

[16] Kenneally, Gavin, Avik De, and Daniel E. Koditschek, "Design Principles for a Family of Direct-Drive Legged Robots", *IEEE Robotics and Automation Letters1* (2), 900-907. January 2016.

[17] Wensing, P. M., A. Wang, S. Seok, D. Otten, J. Lang, and S. Kim, "Proprioceptive actuator design in the MIT cheetah: Impact mitigation and high-bandwidth physical interaction for dynamic legged robots", *IEEE Transactions on Robotics*, 2017.

[18] Seok, S., et al., "Actuator Design for High Force Proprioceptive Control in Fast Legged Locomotion", *Proceedings of the IEEE/RSJ International Conference on Intelligent Robots and Systems*, Vilamoura, Algarve, Portugal, 2012.

[19] Haberland, M., J. Karssen, S. Kim, and M. Wisse, "The effect of swing leg retraction on running energy efficiency," *Proceedings of the IEEE/RSJ International Conference on Intelligent Robots and Systems*, Sept. 2011, pp. 3957 –3962.

[20] Hirosi, S., and Umetani, Y. "The basic Motion Regulation System for a Quadruped Walking Machine", *ASME Paper 80-DET-34*, 1980.

[21] Waldron, KJ, and GL Kinzel. "The relationship between actuator geometry and mechanical efficiency in robots." *Fourth, Symposium on Theory and Practice of Robots and Manipulators*. Poland, 1981.

[22] Song, S-M, and Jong-Kil Lee. "The mechanical efficiency and kinematics of pantograph type manipulators," *Proceeding of the IEEE Int. Conference on Robotics and Automation*, 1988, pp 414–420.

[23] Hubicki, Christian, et al. "Atrias: Enabling agile biped locomotion with a template-driven approach to robot design," *International Journal of Robotics Research*, 2016.

[24] Andy Abate, Ross L Hatton, and Jonathan Hurst. "Passive-dynamic leg design for agile robots," *Proceeding of the IEEE International Conference on Robotics and Automation (ICRA)*, 2015, pp. 4519–4524.

[25] Abate, Andy, Jonathan W. Hurst, and Ross L. Hatton, "Mechanical Antagonism in Legged Robots," *Proceeding of the* Robotics Science and Systems (RSS), June 2016.

[26] Boston Dynamics, (2018, May) "Spot Autonomous Navigation", Available: https://www.youtube.com/watch?v=Ve9kWX_KXus

[27] Machairas, K., and Papadopoulos, E., "Designing gaits of constant forward velocity and body height," *IEEE/RSJ International Conference on Intelligent Robots and Systems (IROS '18)*, Madrid, Spain, October, 1-5, 2018.

[28] https://nereus.mech.ntua.gr/legged/

[29] Dallas, S., Machairas, K., Koutsoukis, K., Papadopoulos, E., "A Leg Design Method for High Speed Quadrupedal Locomotion," *IEEE/RSJ International Conference on Intelligent Robots and Systems (IROS '17)*, Vancouver, BC, Canada, September 24–28, 2017.